Functional Mutation of *SMAC/DIABLO*, Encoding a Mitochondrial Proapoptotic Protein, Causes Human Progressive Hearing Loss DFNA64

Jing Cheng,[1,10] Yuhua Zhu,[1,10] Sudan He,[2,3] Yanping Lu,[4] Jing Chen,[1] Bing Han,[1] Marco Petrillo,[5] Kazimierz O. Wrzeszczynski,[6] Shiming Yang,[1] Pu Dai,[1] Suoqiang Zhai,[1] Dongyi Han,[1] Michael Q. Zhang,[6] Wei Li,[7] Xuezhong Liu,[8] Huawei Li,[9] Zheng-Yi Chen,[5] and Huijun Yuan[1,*]

SMAC/DIABLO is a mitochondrial proapoptotic protein that is released from mitochondria during apoptosis and counters the inhibitory activities of inhibitor of apoptosis proteins, IAPs. By linkage analysis and candidate screening, we identified a heterozygous *SMAC/DIABLO* mutation, c.377C>T (p.Ser126Leu, refers to p.Ser71Leu in the mature protein) in a six-generation Chinese kindred characterized by dominant progressive nonsyndromic hearing loss, designated as DFNA64. SMAC/DIABLO is highly expressed in human embryonic ears and is enriched in the developing mouse inner-ear hair cells, suggesting it has a role in the development and homeostasis of hair cells. We used a functional study to demonstrate that the SMAC/DIABLO^{S71L} mutant, while retaining the proapoptotic function, triggers significant degradation of both wild-type and mutant SMAC/DIABLO and renders host mitochondria susceptible to calcium-induced loss of the membrane potential. Our work identifies DFNA64 as the human genetic disorder associated with SMAC/DIABLO malfunction and suggests that mutant SMAC/DIABLO^{S71L} might cause mitochondrial dysfunction.

Introduction

Hearing loss affects an estimated 28 million Americans, 27.8 million Chinese, and 22.5 million Europeans.[1–3] It was estimated that several-hundred genes could be associated with this sensory deficit in humans. This high genetic heterogeneity could reflect the anatomical and functional complexity of the inner ear. In the past two decades, extensive research efforts on the genetics of hearing loss led to the mapping of 143 loci and the identification of 62 genes responsible for nonsyndromic hearing loss (Hereditary Hearing Loss homepage; see Web Resources). The identification of genes for autosomal-dominant nonsyndromic hearing loss (DFNA) will be important for understanding age-related hearing impairment, the most prominent form of hearing loss. Gene mutations associated with late-onset progressive disorders are most likely to result in less drastic changes in protein structure and function. The progressive nature of these diseases could then be explained by a gradual increase in the ratio of damaged to normal proteins or changes in protein level.[4] The genes involved in human nonsyndromic hearing loss encode proteins with a wide spectrum of biological structures and functions, including transcriptional regulation, K^+ recycling, the cytoskeleton, cell-cell junctions, membrane transport, the extracellular matrix, and other structural components.[5,6]

Loss of hair cells, the auditory sensory cells, by apoptosis is a major cause of hearing loss in mammals.[7–9] A recent study showed that Bak, a proapoptotic protein, is involved in age-related hearing loss in mice.[10] However, none of the 62 human genes involved in nonsyndromic hearing loss is known to have a proapoptotic function. Only *TJP2* (MIM 607709) was recently reported to participate in apoptosis pathways by altering expression of apoptosis genes through genomic duplication and overexpression in DFNA51 (MIM 613558).[11] In 2000, Du et al. identified SMAC (second mitochondria-derived activator of caspase, MIM 605219, accession number AAF87716.1), a proapoptotic mitochondrial protein that promotes caspase activation by relieving IAP inhibition.[12] Verhagen et al. identified the murine homolog of SMAC and named it DIABLO (direct inhibitor of apoptosis protein binding protein with a low pI).[13] SMAC/DIABLO (hereafter referred to as DIABLO, which has been approved by the HUGO Gene Nomenclature Committee) is synthesized as a 239 amino acid precursor molecule. The amino-terminal 55 residues serve as the mitochondria-targeting sequence, which is removed after the Smac protein is imported into mitochondria intermembrane space. Chai et al. determined the crystal structure of DIABLO, which revealed that DIABLO must form a homodimer to interact with IAPs. A particular N-terminal motif, consisting of four amino acids, Ala-Val-Pro-Ile, is responsible for the

[1]Institute of Otolaryngology, Chinese PLA General Hospital, Beijing 100853, China; [2]National Institute of Biological Sciences, No.7 Science Park Road, Zhongguancun Life Science Park, Beijing 102206, China; [3]Cyrus Tang Hematology Center, Jiangsu Institute of Hematology, The First Affiliated Hospital, Soochow University, Suzhou 215325, China; [4]Department of Obstetrics and Gynecology, Chinese People's Liberation Army General Hospital, Beijing 100853, China; [5]Eaton-Peabody Laboratory, Department of Otolaryngology, The Massachusetts Eye and Ear Infirmary, Harvard Medical School, Boston, MA 02114, USA; [6]Michael Zhang Lab, Koch 2124, Computational Biology and Bioinformatics, Cold Spring Harbor Laboratory, 1 Bungtown Road, Cold Spring Harbor, NY 11724, USA; [7]Institute of Genetics and Developmental Biology, Chinese Academy of Sciences, Beijing 100101, China; [8]Department of Otolaryngology, University of Miami, Miami, FL 33136, USA; [9]Department of Otology & Skull Base Surgery, Affiliated Eye and Otolaryngology Hospital of Fudan University, 83 Fenyang Road, Shanghai 200031, China
[10]These authors contributed equally to this work
*Correspondence: yuanhj301@yahoo.com.cn
DOI 10.1016/j.ajhg.2011.05.027.

interaction with IAPs. DIABLO interacts with the BIR2 and BIR3 domains of XIAP, allowing the release of caspase-3 and caspase-9, respectively.[14]

Given its central role in regulating apoptosis, it is expected that DIABLO dysfunction might underlie the pathogenesis of some human diseases. However, no *DIABLO* mutation that is associated with any human genetic disorders has previously been identified. In this paper, we report the identification of a *DIABLO* missense mutation that underlies autosomal-dominant hearing loss, designated as DFNA64, in a six-generation Chinese kindred. We report a functional study to illustrate that the identified mutation causes degradation of mutant and wild-type DIABLO; this degradation is likely to lead to mitochondrial dysfunction and contributes to DFNA64.

Material and Methods

Clinical Evaluations

The family HN-W078 was ascertained from the Henan province of Mainland China. All the procedures were approved by the Ethics Reviewing Committee of the Chinese PLA General Hospital and were carried out only after written informed consent was obtained from each individual and/or parents of the children. The medical history was obtained by use of a questionnaire regarding the following aspects: subjective degree of hearing loss, age at onset, evolution, symmetry of the hearing impairment, hearing aids, presence of tinnitus and vertigo, medication, noise exposure, pathologic changes in the ear, and other relevant clinical manifestations. Otoscopy, physical examination, and pure-tone audiometry (at frequencies from 250 to 8000 Hz) were performed. Immittance testing was applied so that middle-ear functions could be evaluated.

Linkage Analysis

Blood samples (3 ml) were drawn from 33 participants so that genomic DNA could be extracted with the Genomic DNA isolation kit (QIAGEN). A genome-wide scan was performed for a selected 18 subjects via Affymetrix Genome-Wide Human SNP Array 5.0 containing 57,244 SNPs. Multipoint parametric linkage analysis was performed with Merlin v. 1.0 so that parametric LOD scores could be calculated. Penetrance values used for the dominant model were 0.01, 0.90, and 0.90 for the wild-type homozygote, mutant heterozygote, and mutant homozygote, respectively. We assumed a disease allele prevalence frequency of 0.0001 and a phenocopy rate of 1%. Fine mapping was performed with ten microsatellite markers selected from Marshfield chromosome 12 map. The alleles were assigned with Genescan and Genotyper Software (Applied Biosystems, USA). Linkage analysis was performed with the LINKAGE 5.1 software package. The two-point LOD score between the deafness locus and each marker was calculated under a fully penetrant autosomal-dominant mode of inheritance, and the disease allele frequency was set to 0.0001. The meiotic recombination frequencies were considered to be equal for males and females.

Mutation Analysis

Direct sequencing was used for mutation screening. Primers were designed to amplify all exons and flanking intronic splicing sites of genes from genome DNA. Sequences of these primers are given in Table S1, available online. The accession numbers and versions of candidate genes are listed in Table S2.

Quantitative RT-PCR

Expression of *DIABLO* transcript in different human embryonic tissues at week 17 of pregnancy was evaluated by real-time quantitative RT-PCR. All the procedures were approved by the Ethics Reviewing Committee of the Chinese PLA General Hospital. Total RNA was purified with the Trizol method (Invitrogen) and treated with DNase I (QIAGEN). Total RNA (1 μg) was reverse transcribed with the SuperScript III First-Strand Kit (Invitrogen). Amplimer levels were quantified continuously with the SYBR Green system (Applied Biosystems) for analysis of transcript expression of tissues, and the Taq-Man MGB probe system (Applied Biosystems) was applied for the analysis of the transcription of wild-type and mutant *DIABLO* in HeLa cells. Gene expression levels were calculated with the $2^{(-\Delta\Delta CT)}$ method. Target-gene expression was normalized to β-actin expression.

Cell-Viability Assay

Cell-survival analysis was performed with the Cell Titer-Glo Luminescent Cell-Viability Assay kit (Promega) according to manufacturer instruction with minor modification. In brief, 20 μl of Cell Titer-glo reagent was added to the cell culture medium. Luminescent reading was carried on Tecan SpectraFluor Plus reader (Tecan).

Site-Directed Mutagenesis and Recombinant-Protein Preparation

We generated point mutations by using the QuikChange Lightning Site-Directed Mutagenesis Kit (Stratagene).

Immunoprecipitation

Cell lysates were incubated with M2 FLAG agarose beads (Sigma) overnight at 4°C. Beads were washed with lysis buffer containing an additional 300 mM NaCl. The immunoprecipitants were eluted off the beads with low pH elution buffer (Pierce) for 5 min at room temperature. Acid elution was neutralized by the addition of a 1/20 volume of 1 M Tris-HCl (pH 9.4).

Immunolot Analysis

Antibodies were used according to the manufacturer's suggestion. Immunoblot analysis was performed with a horseradish-peroxidase-conjugated goat anti-rabbit immunoglobulin G and enhanced chemiluminescence (ECL) immunoblotting detection reagents (Sigma).

Immunohistochemistry

Mouse inner-ear tissues from timed pregnancy were collected via a previously described procedure.[15] The use of animals and the procedures involving tissue preparation were approved by the Institutional Animal Care and Use Committee of the Massachusetts Eye and Ear Infirmary. Standard procedures were employed for staining cryosectioned mouse cochlear slides and HeLa cells with the antibodies against the following antigens: DIABLO antibody [Y12] (1:200 for HeLa cells, 1:1000 for cochlear slides, Abcam, ab32023), MitoTracker Mitochondrion-Selective Probes (1:5000, Molecular Probe), and DAPI (1× , Molecular Probe).

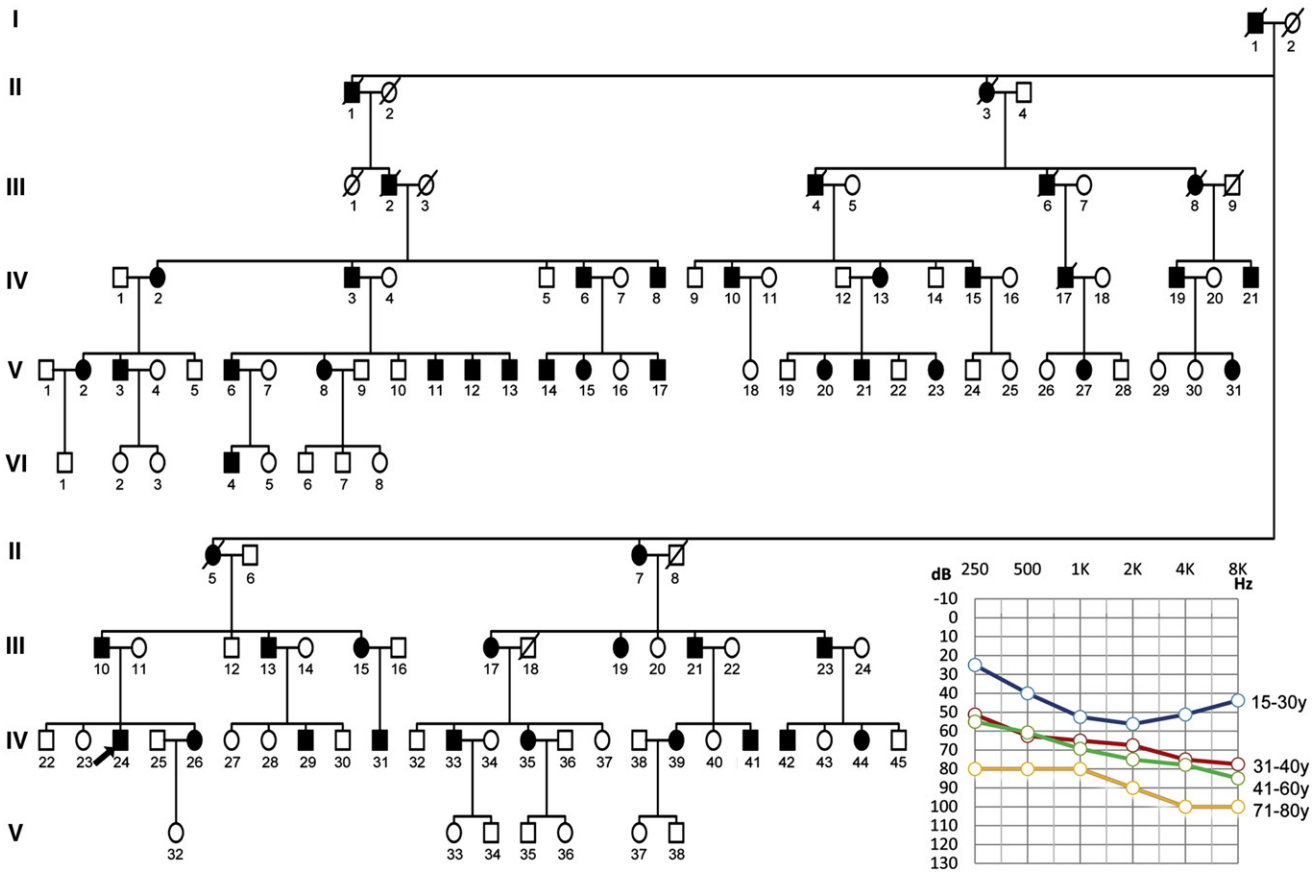

Figure 1. Pedigree of Chinese Family HN-W078 with Dominant Progressive Hearing Loss and a Combined Audiogram of Affected Subjects

Affected subjects are denoted in black. The proband is indicated by an arrow. On the basis of the audiograms of the affected subjects, the severity of hearing impairment appears to be correlated with the individual's age.

Smac-XIAP Binding Assay

Pellet cells were centrifuged from culture media and were washed with phosphate-buffered saline (PBS) and solubilized in 200 μl ice-cold extraction buffer (50 mM HEPES [pH 7.5], 10 mM KCl, 5 mM EGTA, 1 mM $MgCl_2$, 0.2% Chaps, and 0.2 mM DTT) at a density of 2×10^8 cells/ml. The cell pellet was snap frozen in liquid nitrogen and stored at −80°C. Thawed cell were extracted and centrifuged at 14,000 × g for 15 min at 4°C. Then, 10 μl of cell extract was added to tubes containing bovine heart cytochrome c (Sigma, 5 μl of a 1 mg/ml stock), dATP (Sigma, catalog # D6500, 5 μl of a 5.0 mM stock adjusted to pH 7.5 with KOH), and 5 μl of recombinant XIAP protein with or without 5 μl recombinant wild-type and mutant DIABLO. The samples were incubated in a 37°C water bath for 60 min. The cleaved fractions were detected by immunoblot with caspase-3 antibody (Cell signaling, 9662).

Knockdown of Smac by siRNA Transfection

MISSION esiRNAs (Sigma) are endoribonuclease-prepared siRNA pools comprised of a heterogeneous mixture of siRNAs that all target the same mRNA sequence. MISSION siRNA was transfected according to the manufacturer's instructions.

Live-Cell Imaging of Mitochondrial Membrane Permeability

HeLa cells were plated in cultured media (DMEM from Hyclone, 10% FBS, and 1% P/S). Fresh media containing 25 nM TMRM (T668, Invitrogen) and 100 nM mitoTracker Green (M7514, Invitrogen) was added, and incubation followed for 25 min at 37°C under protection from light. Warm media containing 200 μM $CaCl_2$ and 20 μM A23187 (C7522, Sigma) were added. Images were acquired at every 10 min thereafter with a ZEISS 40×/1.42 confocal microscope. Each image was comprised of eight z stacks in which each section was 1 μM in depth.

Results

Family and Clinical Evaluations

The pedigree of family HN-W078, which spans six generations and comprises 127 members, is consistent with an autosomal-dominant inheritance pattern (Figure 1). Thirty-three family members, including 18 affected members and 15 normal individuals, participated in this study. Responses to questionnaires indicated that the age of onset of hearing impairment in this family varied from 12 to 30 years (the average age of onset was 22 years). In 18 affected subjects, hearing impairment was symmetric. The severity of hearing impairment varied from severe to moderate to mild hearing according to the subjects' audiograms. The severity of hearing impairment appears to be correlated with the individual's age

Table 1. Summary of Clinical Data for Some of the Affected Individuals of Family HN-W078

Patient	Gender	Age (Years)		Use of Aminoglycoside	Hearing Test PTA* (dB HL)		Audiogram Shape	Level of Hearing Impairment*	Vertigo	Tinnitus
		At Testing	At Onset		Left Ear	Right Ear				
II:7	female	76	24	no	80	88	flat	severe	no	yes
III:10	male	60	22	no	79	80	flat	severe	no	yes
III:13	male	59	26	no	110	76	flat	severe	no	yes
III:15	female	53	20	no	66	66	flat	moderate	no	yes
III:19	female	52	30	no	60	62	flat	moderate	no	no
IV:3	male	52	24	no	61	68	flat	moderate	no	yes
IV:6	male	49	24	no	63	64	flat	moderate	no	yes
IV:8	male	40	23	no	71	71	flat	severe	no	no
IV:10	male	55	20	no	76	78	flat	severe	no	yes
IV:24	male	30	15	no	70	70	flat	severe	no	yes
IV:26	female	26	20	no	58	55	sloping	moderate	no	yes
IV:31	male	18	12	no	48	48	flat	moderate	no	yes
IV:33	male	33	26	no	60	69	flat	moderate	no	yes
IV:35	female	31	20	no	58	59	flat	moderate	no	yes
V:13	male	27	23	no	53	54	sloping	moderate	no	no
V:27	female	23	16	no	41	44	flat	moderate	no	no

* The degree of hearing loss was defined according to pure-tone averages (PTAs), which were based on the frequencies 500, 1,000, and 2,000 Hz.

(Table 1). Overall, the audiograms of affected members have a flat contour (Figure 1). High-frequency tinnitus was reported in 73% of affected members at the onset of hearing loss. Audiologic evaluation of the family members demonstrated normal immittance testing and bone conduction values that equal the air conduction measurements, suggesting a sensorineural hearing impairment. Comprehensive family medical histories and clinical examination of these individuals showed no other clinical abnormalities, including diabetes, cardiovascular diseases, visual problems, or neurological disorders. Inner-ear malformations were ruled out by computer tomography, which was normal in the proband of this family.

Mapping of DFNA64 Locus

Multipoint genome-wide linkage analysis yielded a positive region with single-nucleotide polymorphism (SNP) markers on chromosome 12q24.31–12q24.32 (chr12: 121,924,854 –128,895,742) between markers rs7955747 and rs10773539 and a maximum logarithm of the odds (LOD) score of 5.66 (Figure 2A). Fine mapping employing extensive microsatellite markers placed a genetic interval between markers D12S86 and D12S1612 (Figure 2B; see also Figure S1). The combination of these two methods allowed us to narrow down the critical interval harboring a candidate locus between the markers rs7955747 and D12S1612, which did not overlap with the flanking DFNA25 (MIM 605583) or DFNA41 (MIM 608224) locus (Figure 2C).[16,17] Thus, we identified a dominant deafness locus, designated as DFNA64 by the Human Genome Organization (HUGO) Gene Nomenclature Committee.

Identification of a Mutation in the DFNA64 Family

The mapped DFNA64 locus spans a physical distance of 3.09 Mb. More than 61 RefSeq genes have been identified in this interval. Sequence analysis of six candidate genes selected from the Morton Cochlear EST Database,[18] *PSMD9* (MIM 603146, 26S proteasome subunit), *CDK2AP1* (MIM 602198, functions in the oncogenic process), *DIABLO* (MIM 605219, functions in the mitochondrial apoptotic pathway), *KDM2B* (MIM 609078, putative tumor suppressor), *ZCCHC8* (gene ID 55596, GSK-3 substrate, functions in RNA metabolism), and *SBNO1* (gene ID 55206, functions in the Notch signaling pathway), led to the identification of a heterozygous C-to-T transition at position 377 in exon 5 (NM_019887.4: c.377 C>T, Figures 2D and 2E). This transition resulted in a p.Ser126Leu (p.Ser71Leu in mature protein) substitution in DIABLO. The Ser residue at position 126 in DIABLO is conserved across human, rat, mouse, bovine, ornithorhynchus, chicken, and *Xenopus* lineages (Figure 2F). EcoR I restriction analysis demonstrated that the c.377 C>T mutation completely cosegregated with hearing loss in family HN-W078 and was absent in 1000 unrelated Chinese control chromosomes. The penetrance of hearing loss in this family is 100% on the basis of the data from investigated

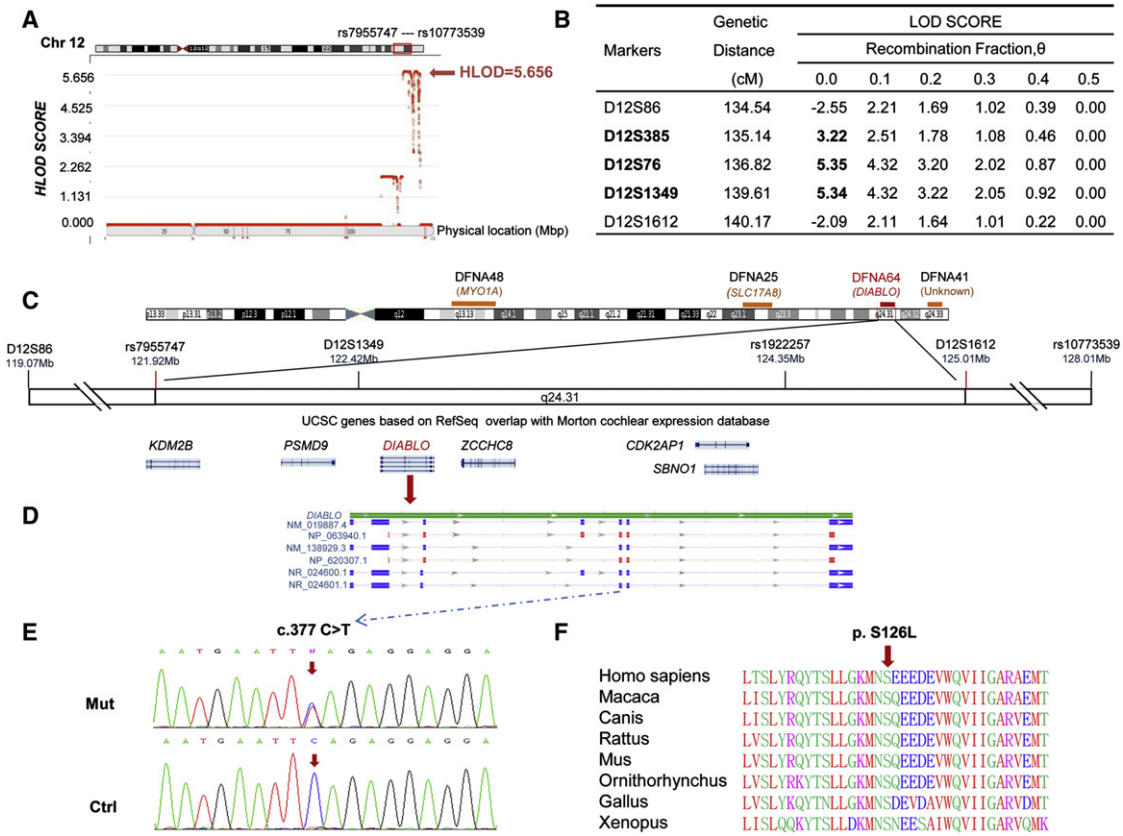

Markers	Genetic Distance (cM)	LOD SCORE Recombination Fraction,θ					
		0.0	0.1	0.2	0.3	0.4	0.5
D12S86	134.54	-2.55	2.21	1.69	1.02	0.39	0.00
D12S385	135.14	**3.22**	2.51	1.78	1.08	0.46	0.00
D12S76	136.82	**5.35**	4.32	3.20	2.02	0.87	0.00
D12S1349	139.61	**5.34**	4.32	3.22	2.05	0.92	0.00
D12S1612	140.17	-2.09	2.11	1.64	1.01	0.22	0.00

Figure 2. Mapping Interval and Mutation Analysis of the Chinese Family HN-W078
(A) Genome-wide linkage analysis with SNP markers defined an interval between markers rs7955747 and rs10773539 and gave a maximum HLOD score of 5.66.
(B) Fine mapping of the candidate region with microsatellite markers defined an interval between markers D12S86 and D12S1612 and gave a maximum LOD score of 5.35.
(C) Idiogram of the DFNA64 locus on chromosome 12 with flanking markers and candidate genes. The loci of DFNA25, DFNA41, and DFNA48 are also indicated.
(D) The genomic structure of different *DIABLO* transcripts. The position of the DFNA64 mutation in exon 5 is shown. *DIABLO* has four different transcripts, but only two of them encode proteins. NM_019887.4 is the longest transcript and encodes NP_063940.1. NM_138929.3 encodes a shorter isoform, NP_620307. Both transcripts harbor exon 5, where the c. 377C>T mutation is located.
(E) DNA sequence chromatograms showing a heterozygous c.377C>T mutation in *DIABLO* in DFNA64 individuals are compared to those of wild-type controls.
(F) Conservation analysis showing that Ser126 in DIABLO is conserved across human, rat, mouse, bovine, ornithorhynchus, chicken, and *Xenopus* lineages.

individuals. All variants identified in six candidate genes in this family are listed in Table S2. We have screened 223 Chinese families or sporadic subjects with late-onset hearing loss (<40 years). We did not find any *DIABLO* mutation in those samples.

DIABLO Is Highly Expressed in the Human and Mouse Inner Ear

To investigate the role of DIABLO malfunction in DFNA64, we first examined the expression of DIABLO in different human embryonic tissues by using real-time quantitative RT-PCR. DIABLO mRNA was detected broadly; the highest expression was in the testis, adrenal gland, and ears, there was moderate expression in the brain, eyes, liver, kidney, lung, and spinal cord, and there was low expression in the spleen (Figure 3A). We next studied the production of Diablo in the developing mouse inner ear with an anti-DIABLO antibody. Diablo was widely expressed at a low level in the developing mouse cochlea (Figure 3C). However, Diablo was significantly upregulated in hair cells from E18.5 to P0 and was subsequently downregulated. A secondary antibody control did not produce any discernable staining pattern (data not shown). The extended distribution of Diablo at different stages of development in the mouse inner ear and the particular enrichment in hair cells suggested that Diablo functions in the development and homeostasis of the inner ear and in hair cells in particular.

Mutant DIABLO Has Similar Proapoptotic Activity to Wild-Type Protein

We carried out bioinformatics analysis to predict the likely functional impact of the DIABLO^{S71L} mutant on the basis of the crystal structure of the wild-type DIABLO

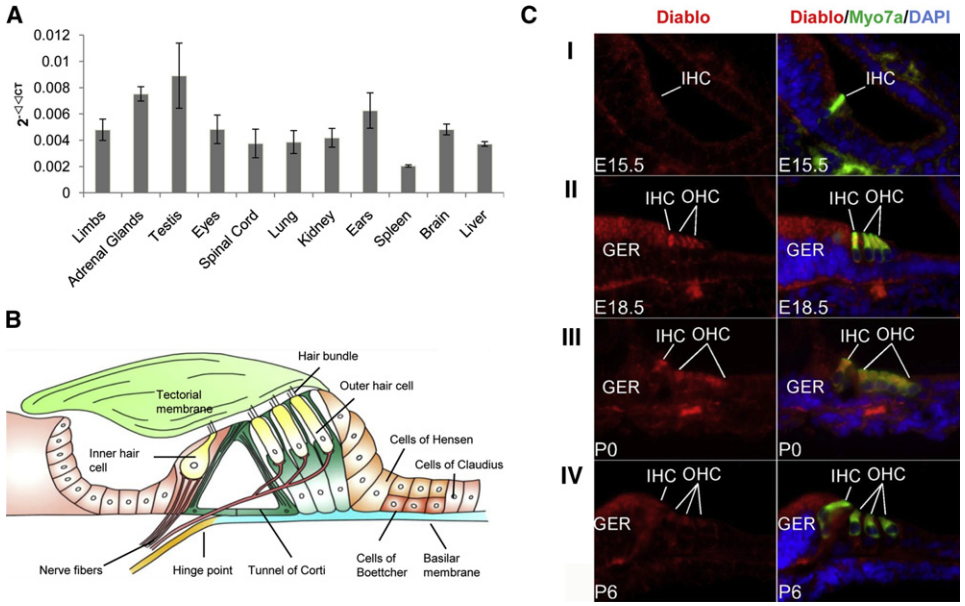

Figure 3. Expression Profiling of DIABLO in the Developing Human and Mouse Inner Ear
(A) Expression of DIABLO transcript in different human embryonic tissues at week 17 of pregnancy was evaluated by real-time quantitative RT-PCR. Data are means ± SD of three independent experiments.
(B) Schematic representation of the Corti's organ in the inner ear. The sensory epithelium of the cochlea consists of inner and outer hair cells. Supporting cells of the Corti's organ include Hensen's, Claudius's, Deiter's, and Boettcher's cells.
(C) Production of DIABLO in the developing mouse cochlea. (I) Cytoplasmic distribution of DIABLO was weakly detected ubiquitously in developing cochlea, including the nascent inner hair cell (IHC) at the base, at E15.5. (II) By E18.5, DIABLO production was significantly elevated in both inner and outer hair cells (IHCs and OHCs), in particular in the cytoplasm above the nuclei. DIABLO was also readily detected in other cell types, including the greater epithelial ridge (GER). (III) DIABLO production was persistently higher in cochlear hair cells at P0 than in surrounding cells. More than three OHCs were present in the image because of the section angle. (IV) By P6, DIABLO was downregulated to a level that was indistinguishable from that of the GER. Myo7a: myosin VIIa that labels hair cells. Magnification: 40×.

(PDB ID: 1FEW). It was indicated that Ser 71 is located at a distance from the XIAP-binding site and on the opposite end of the dimer interface (Figure 4A). Serine 71 might form a hydrogen bond with neighboring Asp 75 and thus stabilize the H1-H2 loop. Disruption of this hydrogen bond could cause protein misfolding or structural damage (data not shown). To test whether the DIABLO^{S71L} mutation would disrupt the DIABLO dimer formation and DIABLO-XIAP binding activity, we expressed human wild-type (DIABLO^{WT}) and mutant DIABLO (DIABLO^{S71L}) in an *E. coli* system. The purified recombinant DIABLO^{S71L} and DIABLO^{WT} showed similar profiles on Sephedex 200 columns and on native polyacrylamide gel electrophoresis (PAGE), indicating that DIABLO^{S71L} is able to form a dimer (Figure 4B). We then investigated DIABLO-XIAP binding activity by assessing caspase 3 activation in an in vitro system. As shown in Figure 4C, procaspase 3 was activated and cleaved into two fragments of P20 and P12 in activated HeLa cell extracts (lane 2); this activity was blocked by the addition of purified recombinant XIAP (lanes 3 and 4). The inhibition of procaspase 3 activation by XIAP was removed by further incubation with DIABLO^{WT} (lanes 5 and 6) or DIABLO^{S71L} (lanes 9 and 10) in a dose-dependent manner. These observations demonstrated that DIABLO^{S71L} does not jeopardize DIABLO-XIAP binding activity. We further investigated the effect of DIABLO^{S71L} mutation on apoptosis in cultured cells. As shown in Figure 4D, HeLa cells overexpressing DIABLO^{WT} or DIABLO^{S71L} showed no significant difference of cell viability when treated with several proapoptotic agents, including etoposide, Actinomycin D, and cisplastin, indicating that DIABLO^{S71L} does not give rise to an increased apoptotic activity under these conditions.

Ectopically Expressed DIABLO^{S71L} Triggered Degradation of the Mutant and Wild-Type DIABLO in a Heterodimeration-Dependent Way in HeLa Cells

To further investigate the effect of DIABLO^{S71L}, we tagged DIABLO^{WT} and DIABLO^{S71L} with FLAG and determined the expression of DIABLO fusion protein in HeLa cells. Similar levels of DIABLO^{WT} and DIABLO^{S71L} mRNA were observed by quantitative real-time RT-PCR analysis (data not shown). Surprisingly, when HeLa cells were transfected with the same amount of DIABLO^{WT} or DIABLO^{S71L} plasmids, the protein level of DIABLO^{S71L} was much lower than that of the DIABLO^{WT} transfected cells. Concurrently with the decreased in DIABLO^{S71L}, the endogenous DIABLO showed a remarkable reduction in HeLa cells transfected with DIABLO^{S71L} as opposed to DIABLO^{WT}. Increasing expression of DIABLO^{S71L} enhanced the degradation of wild-type DIABLO (Figure 5A). These observations were further confirmed by immunohistochemistry

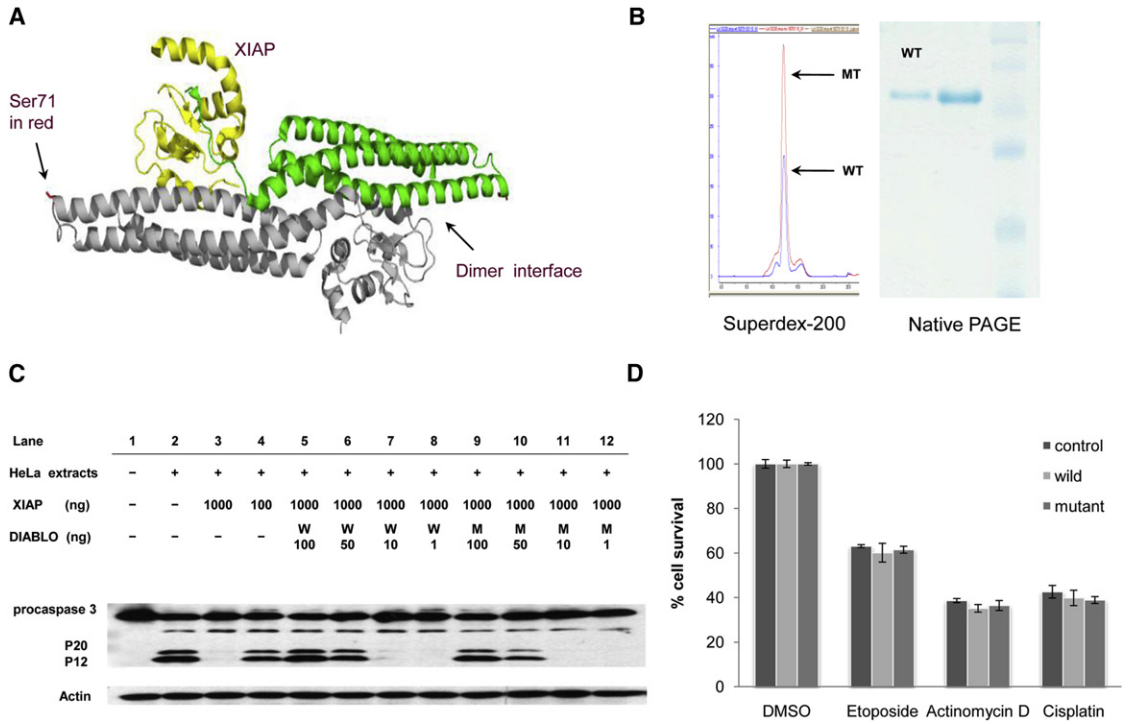

Figure 4. Effects of the DIABLO^{S71L} Mutant on Dimer Formation and DIABLO-XIAP Binding
(A) Structure analysis of the wild-type DIABLO (PDB ID: 1FEW) using PyMol program indicates Ser 71 in mature protein is located at the end of the arch-shaped H1 helix. Binding XIAP is in yellow. The dimer interface is indicated by an arrow.
(B) The purified recombinant DIABLO^{S71L} and DIABLO^{WT} showed the same characters on Sephedex-200 columns and on native polyacrylamide gel electrophoresis (PAGE), indicating that DIABLO^{S71L} is able to form a dimer. WT: wild-type, MT: DIABLO^{S71L} mutant.
(C) DIABLO-XIAP binding activity assay. Procaspase 3 was activated and cleaved into two fragments of P20 and P12 when ctivated HeLa cell extracts (lane 2) were added; this activation and cleavage were blocked by the addition of recombinant XIAP (lanes 3 and 4). The inhibition of procaspase 3 activation by XIAP was removed by the addition of DIABLO^{WT} (lanes 5 and 6) or DIABLO^{S71L} (lanes 9 and 10). Neither 1 nor 10 ng DIABLO^{WT} and DIABLO^{S71L} was enough to antagonize the XIAP effect (lanes 7,8,11, and 12).
(D) Cell-viability assay. In HeLa cells overexpressing DIABLO^{WT} or DIABLO^{S71L}, no difference in cell death was observed after it was triggered by etoposide, Actinomycin D, or cisplatin. Data are represented as mean ± standard deviation of three independent experiments.

(Figure 5B). To determine whether the degradation was specifically induced by the DIABLO^{S71L} mutant, we generated DIABLO^{N70I} and DIABLO^{E72L} constructs and expressed them in parallel with DIABLO^{S71L} in HeLa cells. In contrast to what we observed with the DIABLO^{S71L} mutant, we did not observe the degradation of DIABLO^{N70I}, DIABLO^{E72L} mutants, or endogenous DIABLO in the transfected cells (Figure 5C).

To test whether the degradation of endogenous DIABLO depends on the heterodimer formation of DIABLO^{S71L}-endogenous DIABLO, we generated two constructs with the double mutations DIABLO$^{S71L+V26D}$ and DIABLO$^{S71L+F33D}$, which have a defect in dimerization, as described previously.[14] As shown in Figure 5D, DIABLO^{S71L} as well as DIABLO^{WT} formed dimers with endogenous DIABLO, and two monomeric DIABLO mutants (DIABLO$^{S71L+V26D}$ and DIABLO$^{S71L+F33D}$) were unable to interact with endogenous DIABLO. Consistently, only DIABLO^{S71L} and not DIABLO$^{S71L+V26D}$ or DIABLO$^{S71L+F33D}$ induced the degradation of endogenous DIABLO. These observations demonstrated that the expression of DIABLO^{S71L} in the transfected HeLa cells leads to degradation of both the mutant and endogenous DIABLO through heterodimerization between them.

DIABLO^{S71L} Renders Host Mitochondria Susceptible to Calcium-Induced Loss of Membrane Potential

Active degradation of DIABLO^{S71L} indicates that the mutated protein might trigger mitochondrial stress. Mitochondrial membrane potential ($\Delta\psi$) is a sensitive marker of mitochondrial function, and its reduction has been associated with mitochondrial dysfunction.[19] To assess changes of $\Delta\Psi$ in situ, we used tetramethylrhodamine methyl ester (TMRM), a monovalent cationic fluorescent dye widely used for measuring $\Delta\Psi$.[20,21] In HeLa cells expressing DIABLO^{S71L}, $\Delta\Psi$ rapidly collapsed in response to calcium-induced mitochondria stress, whereas the integrity of mitochondrial structure was preserved, as shown by mitoTracker green staining (Figure 6B). Upon exposure to the same stimuli, cells expressing DIABLO^{WT} exhibited intact $\Delta\psi$ (Figure 6A). We further investigated whether the increased sensitivity to mitochondrial stress was due

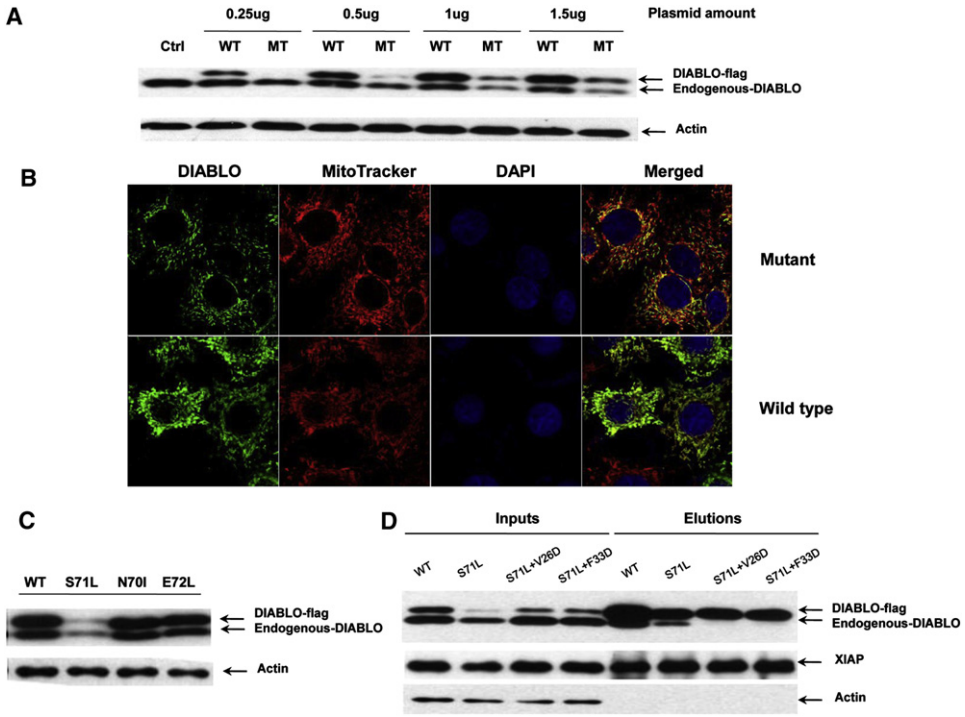

Figure 5. Expression and Degradation of the DIABLO^{S71L} Mutant in HeLa Cells
(A) Immunoblot analysis showed that DIABLO^{S71L} and endogenous DIABLO decreased in a dose-dependent manner in the HeLa cells transfected with DIABLO^{S71L}. Patterns of wild-type and mutant DIABLO did not change.
(B) Immunostaining shows a remarkable reduction of DIABLO in HeLa cells transfected with DIABLO^{S71L}.
(C) DIABLO^{S71L}, DIABLO^{N70I}, and DIABLO^{E72L} mutants and DIABLO^{WT} were expressed in parallel in HeLa cells. The reduction of mutant and endogenous DIABLO was observed only in DIABLO^{S71L}-transfected HeLa cells.
(D) DIABLO^{S71L}, DIABLO$^{S71L+V26D}$, and DIABLO$^{S71L+F33D}$ mutants and DIABLO^{WT} were expressed in HeLa cells. Similar levels of endogenous DIABLO were observed in cells transfected with DIABLO$^{S71L+V26D}$, DIABLO$^{S71L+F33D}$, and DIABLO^{WT}, whereas endogenous DIABLO was decreased only in cells transfected with DIABLO^{S71L}. DIABLO^{S71L}, DIABLO$^{S71L+V26D}$, and DIABLO$^{S71L+F33D}$ mutants were decreased in cell lysates (input, second, third, and forth lanes). Heterodimerization of DIABLO^{S71L} with endogenous DIABLO was indicated by the clear band of endogenous DIABLO in elutions from DIABLO^{S71L}-FLAG-agarose beads (elution, second lane). There was no detectable endogenous DIABLO pulled down from cells transfected with DIABLO$^{S71L+V26D}$ and DIABLO$^{S71L+F33D}$ (elution, third and forth lanes). XIAP was detected in both inputs, and elutions confirmed that DIABLO^{S71L}, DIABLO$^{S71L+V26D}$, and DIABLO$^{S71L+F33D}$ mutants bound to XIAP normally.

to the expression of DIABLO^{S71L} or to the loss of endogenous DIABLO. As shown in Figure 6C, expression of DIABLO$^{S71L+V26D}$ caused cells to lose $\Delta\psi$, which was similar to what occurred in the DIABLO^{S71}-transfected cells, whereas a significant decrease in the endogenous DIABLO by RNA interference (Figure S2) had no effect on $\Delta\psi$ (Figure 6D). These results strongly suggest that the impairment of mitochondrial membrane potential in the HeLa cells transfected with DIABLO^{S71L} is specifically caused by the existence of DIABLO^{S71L}, leading to the activation of a degradation machinery for constant clearance of aberrant proteins.

Discussion

In the present study, a heterozygous missense mutation, c.377C>T, that is genetically linked to progressive, nonsyndromic, sensorineural hearing loss in an extended Chinese DFNA64 family was identified in *DIABLO*. Because of the critical role of DIABLO in the apoptosis pathway, it was tempting to speculate that the pathological mechanism of DFNA64 might be associated with a gain of function in apoptosis in the inner ear. The possible gain of function of apoptosis could be mediated by the following mechanisms: (1) the DIABLO^{S71L} mutant enhances the binding of XIAP-DIABLO; (2) the normal degradation of DIABLO is disrupted by the mutation, increasing the protein level of DIABLO^{S71L}; or (3) the DIABLO^{S71L} mutant enhances IAP auto-ubiquitination, increasing the degradation of IAPs. To test these hypotheses, we overexpressed both wild-type and mutant DIABLO in HeLa cells and used a cell-viability assay to compare their effects on apoptosis. We did not detect discernable differences in cell death induced by mutant or wild-type DIABLO. This is consistent with the prediction by molecular modeling that the p.Ser71Leu mutation is located at the end of the arch-shaped H1 helix, far away from the binding site of DIABLO-IAPs and the dimer interface, and thus might not impact the apoptotic function of DIABLO significantly.

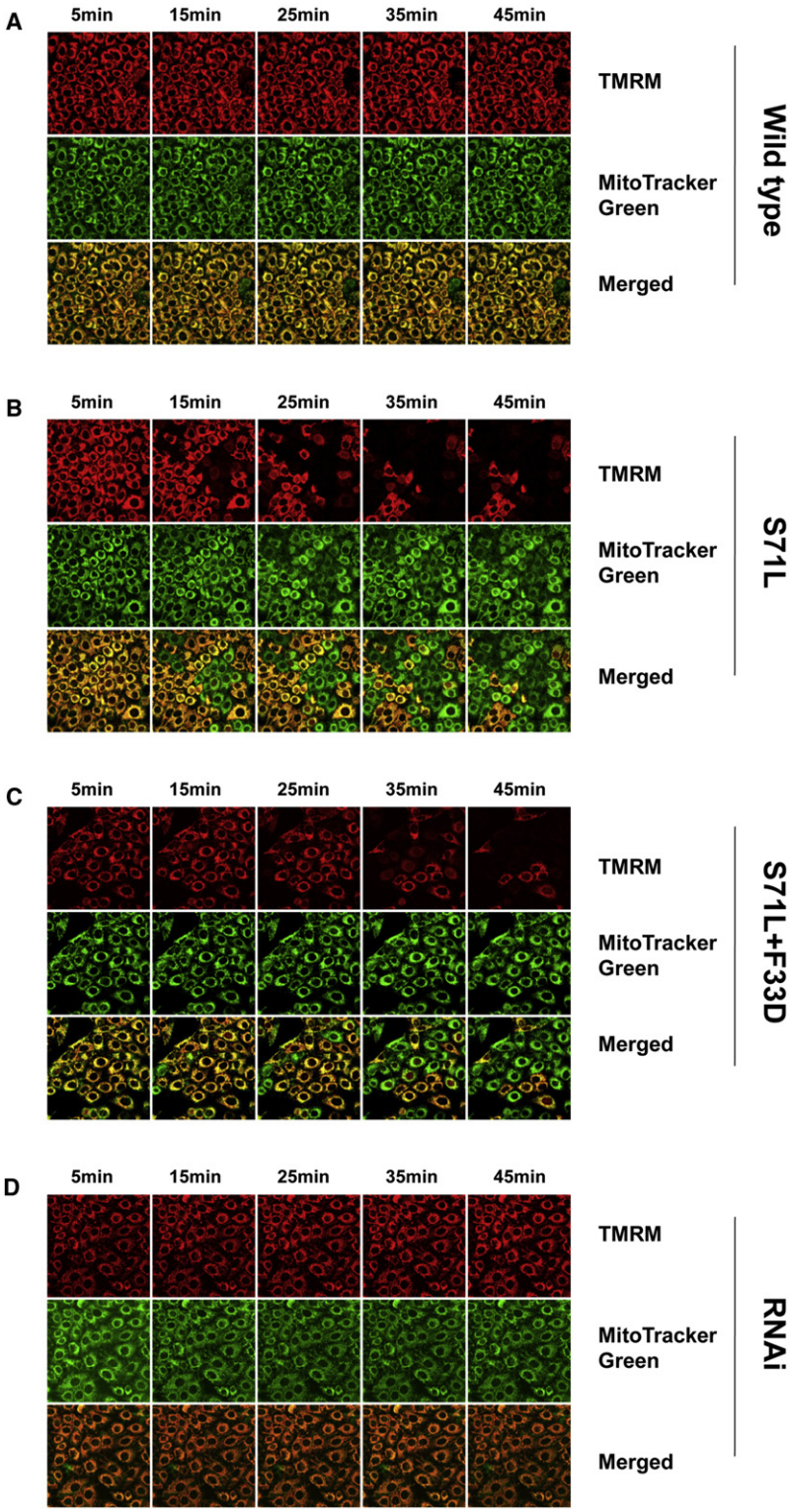

Figure 6. Mitochondrial Membrane-Potential Assay

In HeLa cells transfected with DIABLO^{WT}, DIABLO^{S71L}, DIABLO$^{S71L+V26D}$, and siRNA, mitochondrial membrane potential was monitored by the loss of tetramethylrhodamine methyl ester (TMRM) fluorescence after exposure to the calcium ionophore A23187.

(A and C) Mitochondrial membrane potential was preserved for at least 45 min after exposure to A23187 in DIABLO^{WT} and siRNA transfection.

(B and D) In HeLa cells expressing DIABLO^{S71L} or DIABLO$^{S71L+V26D}$, a loss of mitochondrial membrane potential was observed 15–45 min after exposure to A23187. The integrity of mitochondrial structure was shown by immunostaining with mitoTracker green. Experiments were replicated three times with similar results.

DIABLO by in immunoblot analysis. In contrast, the protein level of DIABLO^{S71L} decreased with the time of expression. Moreover, the endogenous wild-type DIABLO was degraded in the DIABLO^{S71L}-expressing HeLa cells, and the degradation of DIABLO^{WT} is dependent on DIABLO^{S71L}-DIABLO^{WT} dimerization. Although the mechanism underlying degradation is yet to be determined, these results demonstrate that the DIABLO^{S71L} mutant exhibits a specific deleterious effect that can be recognized and cleared by host cells, and such an effect extends to native wild-type DIABLO as a result of dimerization with the mutant protein, leading to severe reduction of the overall DIABLO level.

By quantitative RT-PCR and immunohistochemistry, we have shown that DIABLO was highly expressed in the human embryonic inner ear and that the protein level was elevated in the developing mouse hair cells; these results are consistent with the potential function of DIABLO in mammalian inner-ear development and maintenance. The inner ear is a delicate organ with a limited number of postmitotic hair cells, whose differentiation and maturation state has to be precisely controlled, both for their survival and normal function. This is demonstrated by a disproportionally large number of hair cell genes in which mutations cause hair cell developmental defects, malfunction, or cell death, leading to hearing loss.

An alternative hypothesis is that DFNA64 might be caused by an accumulation of DIABLO^{S71L} protein that forms aggregates in hair cells. Such a mechanism has been described in neurodegenerative disorders, including Alzheimer, Huntington, and Parkinson diseases.[22] However, overexpression of the DIABLO^{S71L} mutant in HeLa cells did not lead to an increased level of aberrant

Mitochondria assume central functions, including ATP production, calcium homeostasis, reactive oxygen species generation, and apoptotic signaling, in cells. Inner-ear hair cells and neurons are particularly dependent upon proper mitochondrial function to support high-energy

demand and cell maintenance. Smith and colleagues demonstrated that vulnerable neurons in the brains of individuals with Alzheimer disease have increased mitochondrial degradation products, suggesting a greater turnover of mitochondria by autophagy and/or a reduction of proteolytic turnover and resulting accumulation of products of mitochondrial degradation.[23] In mouse models, age-related hearing loss has been associated with an accumulation of oxidative stress induced by reactive oxygen species (ROS); mitochondria are a major source of ROS generation and the site of ROS-induced damage.[24] Given our evidence that DIABLO^{S71L} collapses the mitochondrial membrane potential under stress and that DIABLO^{S71L} is associated with progressive hearing loss in the family studied, it is highly likely that the defects caused by DIABLO^{S71L} might ultimately result in chronical mitochondrial dysfunction and thus lead to hair cell degeneration and death. Because hair cells are long-lived terminally differentiated cells, in vivo expression of DIABLO^{S71L} is likely to be less dramatic, and the defects associated with DIABLO^{S71L} will probably be subtle and accumulative and only become pathological over time. This hypothesis is consistent with the late onset and progressive nature of hearing impairment in DFNA64. A mouse model that expresses a mutant allele of DIABLO^{S71L} in a DIABLO^{wt} background will be the next tool in the study of accumulative effects and progressive hearing loss. Furthermore, it remains to be determined which degradation pathway DIABLO^{S71L} activates.

Unveiling new molecular mechanisms of hearing impairment might result in valuable insights into the molecular triggers for hair cell degeneration and provide the basis for genetic diagnosis as well as exciting developments in therapeutic intervention in hearing loss. Work pioneered by Steven McKnight has shown that proneurogenic chemical P7C3 is able to preserve mitochondrial membrane permeability by a yet unknown mechanism.[21] Our results raise the possibility of utilizing mitochondria protective compound (such as P7C3) for potential therapeutic benefit to protect hair cell mitochondrial membrane potential and attenuate the progression of hearing loss in DFNA64 individuals. This would represent a new direction for possible intervention in progressive hearing loss among the general deaf population.

Supplemental Data

Supplemental Data includes two figures and two tables and can be found with this article online at http://www.cell.com/AJHG/.

Acknowledgments

We sincerely thank Xiaodong Wang for extensive help in invaluable scientific input and manuscript revision, Xue Zhang and Hui Jiang for helpful discussions, and Yueshuai Song and Chunhua Xu for technical assistance with the figure preparation and graphical artwork. These investigations were supported by grants from the National High Technology Research and Development Program of China (863 Program, 2007AA02E466) and the Key Project of National Natural Science Foundation of China (81030017) to H.J.Y., grants from the National Natural Science Foundation of China (30728030) and National Institutes of Health (R01 DC006908) to Z.Y.C., a grant from the Fredrick and Ines Yeatts Inner Ear Hair Cell Regeneration Fellowship to M.P., a grant from the National Institutes of Health (R01 DC05575) to X.Z.L., and a grant from the Chinese National Programs for Fundamental Research and Development (973 Program, 2011CB504506) to H.W.L. We thank all the family members for their participation and support in this study.

Received: March 16, 2011
Revised: May 3, 2011
Accepted: May 25, 2011
Published online: June 30, 2011

Web Resources

The URLs for data presented herein are as follows:

dbSNP, http://www.ncbi.nlm.nih.gov/SNP/
GenBank, http://www.ncbi.nlm.nih.gov/Genbank/
Hereditary Hearing Loss homepage, http://hereditaryhearingloss.org
HUGO Gene Nomenclature Committee, http://www.genenames.org
Marshfield chromosome map, http://research.marshfieldclinic.org/genetics
Morton Cochlear EST Database, http://www.brighamandwomens.org/bwh_hearing/human-cochlear-ests.aspx
Online Mendelian Inheritance in Man (OMIM), http://www.ncbi.nlm.nih.gov/Omim/
PyMOL, http://pymol.org/
UCSC Genome Browser, http://genome.ucsc.edu/cgi-bin/hgGateway

References

1. Liu, X.Z., and Yan, D. (2007). Ageing and hearing loss. J. Pathol. *211*, 188–197.
2. Dror, A.A., and Avraham, K.B. (2009). Hearing loss: Mechanisms revealed by genetics and cell biology. Annu. Rev. Genet. *43*, 411–437.
3. Sun, X.B., Wei, Z.Y., Yu, L.M., Wang, Q., and Liang, W. (2008). [Prevalence and etiology of people with hearing impairment in China]. Zhonghua Liu Xing Bing Xue Za Zhi *29*, 643–646.
4. Petersen, M.B. (2002). Non-syndromic autosomal-dominant deafness. Clin. Genet. *62*, 1–13.
5. Resendes, B.L., Williamson, R.E., and Morton, C.C. (2001). At the speed of sound: gene discovery in the auditory system. Am. J. Hum. Genet. *69*, 923–935.
6. Steel, K.P., and Kros, C.J. (2001). A genetic approach to understanding auditory function. Nat. Genet. *27*, 143–149.
7. Lallemend, F., Lefebvre, P.P., Hans, G., Moonen, G., and Malgrange, B. (2005). Molecular pathways involved in apoptotic cell death in the injured cochlea: Cues to novel therapeutic strategies. Curr. Pharm. Des. *11*, 2257–2275.
8. Nicotera, T.M., Hu, B.H., and Henderson, D. (2003). The caspase pathway in noise-induced apoptosis of the chinchilla cochlea. J. Assoc. Res. Otolaryngol. *4*, 466–477.
9. Van De Water, T.R., Lallemend, F., Eshraghi, A.A., Ahsan, S., He, J., Guzman, J., Polak, M., Malgrange, B., Lefebvre, P.P.,

Staecker, H., and Balkany, T.J. (2004). Caspases, the enemy within, and their role in oxidative stress-induced apoptosis of inner ear sensory cells. Otol. Neurotol. *25*, 627–632.
10. Someya, S., Xu, J., Kondo, K., Ding, D., Salvi, R.J., Yamasoba, T., Rabinovitch, P.S., Weindruch, R., Leeuwenburgh, C., Tanokura, M., and Prolla, T.A. (2009). Age-related hearing loss in C57BL/6J mice is mediated by Bak-dependent mitochondrial apoptosis. Proc. Natl. Acad. Sci. USA *106*, 19432–19437.
11. Walsh, T., Pierce, S.B., Lenz, D.R., Brownstein, Z., Dagan-Rosenfeld, O., Shahin, H., Roeb, W., McCarthy, S., Nord, A.S., Gordon, C.R., et al. (2010). Genomic duplication and overexpression of TJP2/ZO-2 leads to altered expression of apoptosis genes in progressive nonsyndromic hearing loss DFNA51. Am. J. Hum. Genet. *87*, 101–109.
12. Du, C., Fang, M., Li, Y., Li, L., and Wang, X. (2000). Smac, a mitochondrial protein that promotes cytochrome c-dependent caspase activation by eliminating IAP inhibition. Cell *102*, 33–42.
13. Verhagen, A.M., Ekert, P.G., Pakusch, M., Silke, J., Connolly, L.M., Reid, G.E., Moritz, R.L., Simpson, R.J., and Vaux, D.L. (2000). Identification of DIABLO, a mammalian protein that promotes apoptosis by binding to and antagonizing IAP proteins. Cell *102*, 43–53.
14. Chai, J., Du, C., Wu, J.W., Kyin, S., Wang, X., and Shi, Y. (2000). Structural and biochemical basis of apoptotic activation by Smac/DIABLO. Nature *406*, 855–862.
15. Sage, C., Huang, M., Karimi, K., Gutierrez, G., Vollrath, M.A., Zhang, D.S., García-Añoveros, J., Hinds, P.W., Corwin, J.T., Corey, D.P., and Chen, Z.Y. (2005). Proliferation of functional hair cells in vivo in the absence of the retinoblastoma protein. Science *307*, 1114–1118.
16. Greene, C.C., McMillan, P.M., Barker, S.E., Kurnool, P., Lomax, M.I., Burmeister, M., and Lesperance, M.M. (2001). DFNA25, a novel locus for dominant nonsyndromic hereditary hearing impairment, maps to 12q21-24. Am. J. Hum. Genet. *68*, 254–260.
17. Blanton, S.H., Liang, C.Y., Cai, M.W., Pandya, A., Du, L.L., Landa, B., Mummalanni, S., Li, K.S., Chen, Z.Y., Qin, X.N., et al. (2002). A novel locus for autosomal dominant non-syndromic deafness (DFNA41) maps to chromosome 12q24-qter. J. Med. Genet. *39*, 567–570.
18. Skvorak, A.B., Weng, Z., Yee, A.J., Robertson, N.G., and Morton, C.C. (1999). Human cochlear expressed sequence tags provide insight into cochlear gene expression and identify candidate genes for deafness. Hum. Mol. Genet. *8*, 439–452.
19. Veatch, J.R., McMurray, M.A., Nelson, Z.W., and Gottschling, D.E. (2009). Mitochondrial dysfunction leads to nuclear genome instability via an iron-sulfur cluster defect. Cell *137*, 1247–1258.
20. Distelmaier, F., Koopman, W.J., Testa, E.R., de Jong, A.S., Swarts, H.G., Mayatepek, E., Smeitink, J.A., and Willems, P.H. (2008). Life cell quantification of mitochondrial membrane potential at the single organelle level. Cytometry A *73*, 129–138.
21. Pieper, A.A., Xie, S., Capota, E., Estill, S.J., Zhong, J., Long, J.M., Becker, G.L., Huntington, P., Goldman, S.E., Shen, C.H., et al. (2010). Discovery of a proneurogenic, neuroprotective chemical. Cell *142*, 39–51.
22. Williams, A., Jahreiss, L., Sarkar, S., Saiki, S., Menzies, F.M., Ravikumar, B., and Rubinsztein, D.C. (2006). Aggregate-prone proteins are cleared from the cytosol by autophagy: Therapeutic implications. Curr. Top. Dev. Biol. *76*, 89–101.
23. Zhu, X., Perry, G., Moreira, P.I., Aliev, G., Cash, A.D., Hirai, K., and Smith, M.A. (2006). Mitochondrial abnormalities and oxidative imbalance in Alzheimer disease. J. Alzheimers Dis. *9*, 147–153.
24. Orrenius, S., Gogvadze, V., and Zhivotovsky, B. (2007). Mitochondrial oxidative stress: implications for cell death. Annu. Rev. Pharmacol. Toxicol. *47*, 143–183.